NUMERICAL SIMULATION OF TSUNAMI IMPACT FROM THE 1/15/22 ERUPTION OF THE HUNGA TONGA - HUNGA HA'APAI VOLCANO

Stephan Grilli, grilli@uri.edu, Maryam Mohammadpour, mmohammadpour@uri.edu, Annette Grilli, annette_grilli@uri.edu
Ocean Engineering Department, University of Rhode Island, USA
Cheng Zhang, Princeton University, USA, chzhang@udel.edu
Dave Tappin, drta@bgs.ac.uk, Alessandro Novellino, alessn@bgs.ac.uk, British Geological Survey, Nottingham, UK
Sebastien Watt, University of Birmingham, Birmingham, UK, S.Watt@bham.ac.uk

OVERVIEW

Tsunamis from volcanic 'explosive' eruptions are rare, with the last catastrophic event being Krakatau in 1883 (Verbeek, 1885), during which, tsunamis were generated in the far-field by pressure shock-waves and in the near-field of the volcano, in the Sunda Straits, by several potential geological mechanisms including pyroclastic flows, ash column, and/or caldera collapse.

On 1/22/55, at about 4:15 UTC, a one in 1,000 year eruption of the Hunga Tonga-Hunga Ha'a-pai Volcano (HTHHV; Fig. 1a), that had started on12/20/21, reached its paroxysm with a series of large underwater explosions, releasing enormous energy (4-18 Mt of TNT), and ejecting a large ash plume 58 km into the stratosphere. Yuen et al. (2022) detail the unfolding of this complex event and the vast amount of diverse data that were measured. During this paroxysmal stage, the combined effects of the underwater explosions and the atmospheric pressure (Lamb) shock-waves these produced (Adam, 2022), generated large tsunamis. In the near-field, within 10-15 minutes, waves with a reported 15+ m flow depth at the shore caused extensive destruction, southward, along the NW coast of Tongatapu and, eastward, in the Ha'apai islands (Figs. 1a,b). The pressure Lamb waves propagated radially away from the volcano, at the speed of sound, while decaying (Amores et al., 2022), and generated additional "meteotsunamis" (MTs) that arrived at far-field pressure/tide gauges ahead of the explosion-generated tsunami. In the deepest areas of the Pacific Ocean (e.g., the 10,000 m deep Kermadec Trench; Fig. 1a), where a complete-to-partial Proudman (1929) resonance occurred, these MTs were amplified, causing a larger far-field impact at some locations (e.g., Lynett et al., 2022).

METHODS AND RESULTS

We simulate both the near- and far-field tsunami generation from the eruption, but in this paper we focus on analyzing and validating the near-field impact against field data. As we shall see, the tsunami wave-train was highly dispersive near the source, which required performing simulations using a dispersive wave model, here, the fully nonlinear Boussinesq Model FUNWAVE-TVD, which features extended dispersion properties (Shi et al., 2012; Kirby et al., 2013). We used nested grids, with one Cartesian grid in the near-field (50 m resolution) (Fig. 1a) and three nested spherical coordinate (0.25, 0.5 and 2 arc-min) grids to simulate the far-field in the Pacific Ocean. Bathymetry was interpolated from several sources, including high-resolution data in Tonga (Borrero, pers. communication) and around HTHHV. We modeled explosion tsunami sources ranging from 3 to 10 Mt, with an initial surface elevation defined using a semi-empirical method, similar to Hayward et al. (2022) (Fig. 1c). We

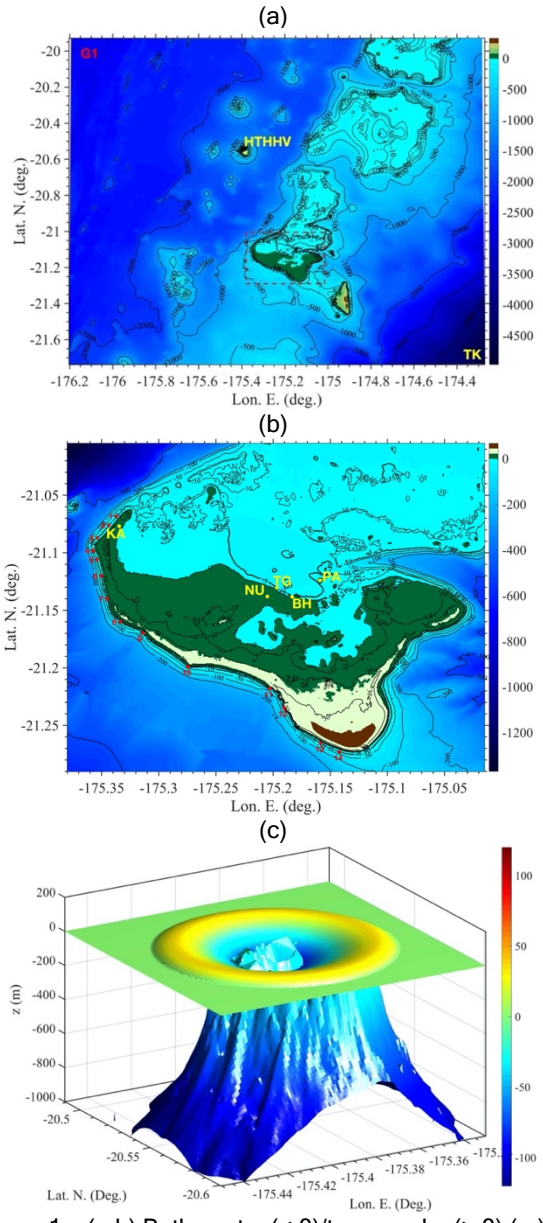

Figure 1 – (a,b) Bathymetry (< 0)/topography (> 0) (m) in 50 m Cartesian FUNWAVE grid; dashed box in (a) is zoom-in area of (b) on Tongatapu. With: HTHHV: volcano location; TK: Tonga-Kermadec arc; (KA) Kanokupolu, (NU) Nuku'alofa; (TG) NU tide gauge; (BH) Boat Harbor; and (PA) Pangaimotu Island; red dots in (b) mark locations of numerical gauges in 10-15 m depth. (c) Initial surface elevation (source) for a 3 Mt explosion occurring at HTHHV at 4:20 UTC.

model the pressure pulse/shockwave as an expanding N-wave, whose pressure gradient forces the model (in space and time). The N-wave is parameterized based on meteorological data measured at 134 stations (Lynett, 2022). Results show, however, that only the static pressure significantly affects the tsunami in the near-field.

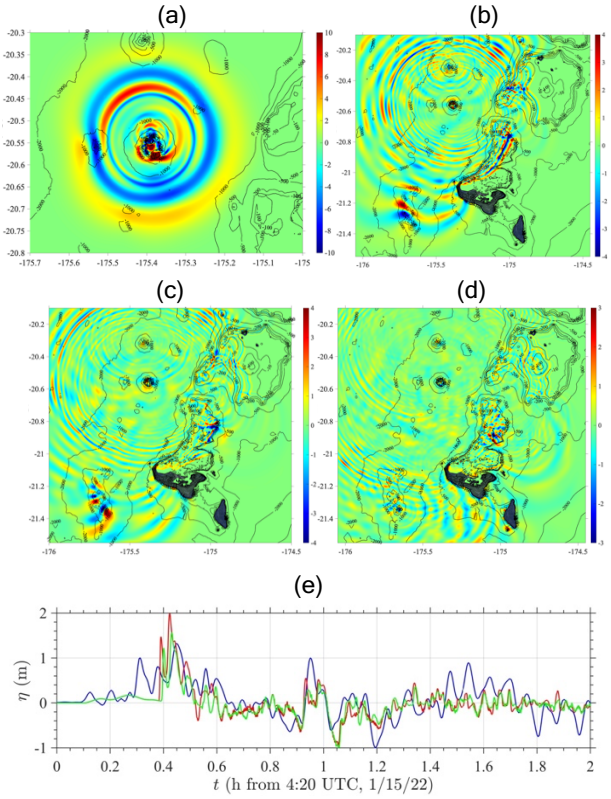

Figure 2 – (a-d) Tsunami elevation (meter) simulated with FUNWAVE-TVD for a 3 Mt explosion of HTHHV (Fig. 1b), in 50 m resolution grid (Fig. 1a) after: (a) 2'30"; (b) 15'; (c) 20'; (d) 30' (referred to 4:20 UTC). (e) Surface elevation time series at Tongatapu's Nuku'alofa tide gauge (Fig. 1c) computed for a: (green) 3 Mt and (red) 5 Mt explosion, with the addition of the static pressure pulse effect, compared to the measured data (blue).

Figs. 2a-d show some computed instantaneous surface elevations, which confirm the highly dispersive nature of the wavetrain. In Fig. 2b, after 15', we see that the NW shore of Tongatapu has already been overtopped and in Fig. 2d, after 30', the coastline of the entire island has been impacted by the near-field tsunami. In Fig. 2e, we compare modeled and measured time series of surface elevations at a tide gauge located in Nuku'alofa on Tongatapu (TG in Fig. 1b). This shows that the tsunami from a 3Mt explosion triggered at 4:20 UTC can explain the data quite well (both elevation and phase), which is consistent with many observations and reports that the largest explosion occurred at 4:16-17 UTC and took about 3 min to develop. Along the NW shore of Tongatapu, the 3Mt simulations predict a maximum flow depth of 16.5 m (Fig. 3) near Kanokupolu (KA in Fig. 1b) and, at other locations along the island's shore, in particular the south and east shores, and around the Boat Harbor and Pangaimotu Island t(BH and PA in Fig. 1b), the predicted flow depths agree well with field survey reports (Cronin, personal communication).

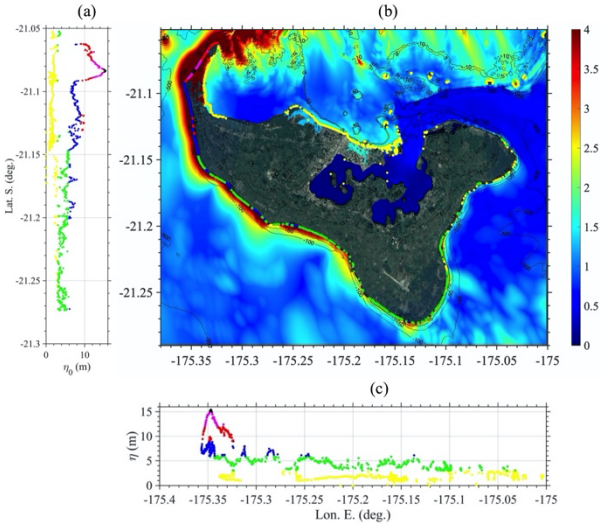

Figure 3 – Zoom-in of tsunami simulations in dashed box in Fig. 1a: (b) Envelope of maximum surface elevation (colorscale in m) computed on Tongatapu's NW coast, after 2 h of simulations, for a 3 Mt explosion source (Fig. 1b); (a,c) Color-coded flow depth along the shore: (< 3 m (yellow); 3-6 m (green); 6-9 m (blue); 9-12 m (red); 12-15 m (purple); > 15 m (black)).

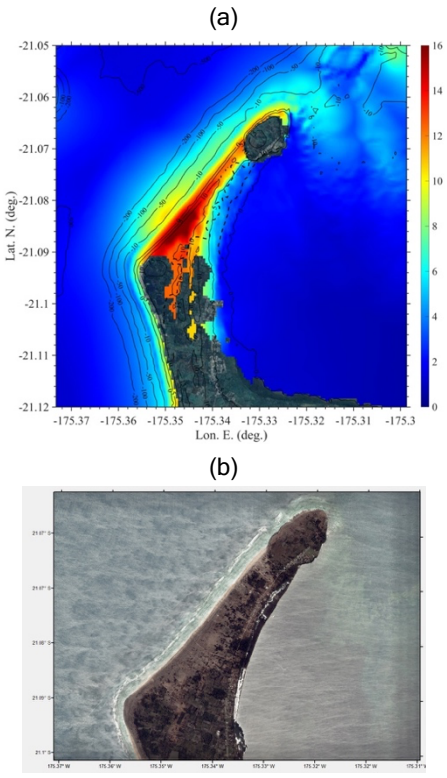

Figure 4 – Zoom in Fig. 3 on NW shore of Tongatapu: (a) Computed envelope of maximum surface elevation (m). (b) Post-tsunami satellite image of the same area.

In particular, consistent with field and satellite observations, the maximum flow depth is predicted at 15-16.5 m on the NW shore of Tongatapu near Kanokupolu (Fig. 3a); this part of the island was overtopped by the tsunami, as can be seen in a post-tsunami satellite image (Fig. 3b). Simulating a larger explosion of 5 Mt, we find that this overestimates the largest waves measured both at the tide gauge (Fig. 2e) and also the overtopping of the NW part of the island (18-20 m flow depth; not shown here). A 10 Mt explosion would create an even larger tsunami with impact that does not agree at all with observations.

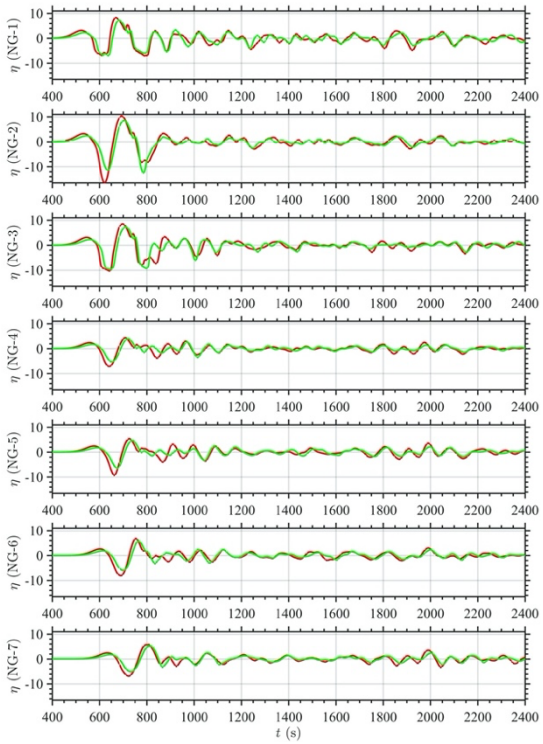

Figure 5 – Time series of surface elevation (m) computed at numerical wave gauges 1-7 in 10-15 m depth (Fig. 1b): (green) 3 Mt, or (red) 5 Mt explosion.

Finally, Fig. 5 shows time series of surface elevation (m) computed at numerical wave gauges 1-7, located in 10 m depth off the NW coast of Tongatapu, where maximum tsunami impact occurred. These show long dispersive incident wave trains with, for 3Mt, waves leading waves of over ~20 m height and a ~3' period.

Far-field tsunamis from our dual source modeling, similar to Lynett et al. (2022), are also found to agree well with measurements made at DART and other pressure sensors (Kubota et al., 2022); selected results will be shown at the conference. At such sensors, the surface elevation caused by the Lamb wave static pressure pulse is first measured, followed by wavetrains that arrive ahead of the explosion-generated tsunami, directly propagating from HTHHV, in some cases by as much as 2-3 h. These early waves result from additional MT generation that is amplified through Proudman resonance, particularly, in deeper water areas where the long wave speed is close to that of the Lamb wave (about 310 m/s or the long wave that occurs in 10,000 m depth).

CONCLUSIONS

Overall, our simulation results indicate that the proposed explosion-generated tsunami mechanism, from the largest explosion (assuming that 3 Mt of energy was transferred to the near-field tsunami) that occurred during the culmination of the eruption, explains well the available near-field observations. The main generation mechanism, hence, does not appear to via mass displacement on the seafloor, such as from underwater flank and/or caldera collapse, or due to the collapse of the ash column, as the timing of and wave generation from these mechanisms would have been very different, but is explosion driven. This explosion probably occurred when seawater interacted with ascending magma during the onset of the main explosive phase of the eruption.

These observations and results also show that the tsunami mechanisms for a large volume caldera collapse, such as during Krakatau 1883 where it was associated with a much larger explosion (Verbeek, 1885), O(150-200) Mt, require re-evaluation. The HTHHV eruption provides the first opportunity since Krakatau to assess whether the proposed tsunami mechanisms are valid (Terry et al., 2022).

REFERENCES

Adam, D. (2022). Tonga volcano eruption created puzzling ripples in Earth's atmosphere. Nature, 601, 497.

Amores, Monserrat, Marcos, Argüeso, Villalonga, Jordà, Gomis (2022). Numerical simulation of atmospheric Lamb waves generated by the 2022 Hunga-Tonga volcanic eruption. Geophys. Res. Lett., e2022GL098240

Hayward, Whittaker, Lane, Power, Popinet, White (2022). Multilayer modelling of waves generated by explosive subaqueous volcanism. Nat. Haz. Earth Syst. Sci., 22(2), 617-637.

Kirby, Shi, Tehranirad, Harris, Grilli (2013). Dispersive tsunami waves in the ocean: Model equations and sensitivity to dispersion and Coriolis effects. Oc. Model., 62, 39-55.

Kubota T., Saito T. and K. Nishida (2022). Global fast-traveling tsunamis by atmospheric pressure waves on the 2022 Tonga eruption. Science, 377(6601), 91-94.

Lynett et 17 Alii (2022). The Tsunamis Generated by the Hunga Tonga-Hunga Ha'apai Volcano on Jan. 15, 1 2022, Nature, https://doi.org/10.1038/s41586-022-05170-6.

Proudman, J. (1929). The effects on the sea of changes in atmospheric pressure, Geophys. Suppl. Mon. Notices R. Astron. Soc., 2(4), 197- 209.

Shi F., Kirby J.T., Harris J.C., Geiman J.D. and S.T. Grilli (2012). A High-Order Adaptive Time-Stepping TVD Solver for Boussinesq Modeling of Breaking Waves and Coastal Inundation. Ocean Modeling, 43-44, 36-51.

Terry, J.P., Goff, J., Winspear, N., Bongolan, V.P., Fisher, S. (2022). Tonga volcanic eruption and tsunami, January 2022: globally the most significant opportunity to observe an explosive and tsunamigenic submarine eruption since AD 1883 Krakatau. Geoscience Letters 9, 24.

Verbeek, R.D.M. (1885). Krakatau. Government Press Batavia.

Yuen and XIV Alii (2022). Under the Surface: Pressure-Induced Planetary-Scale Waves, Volcanic Lightning, and Gaseous Clouds Caused by the Submarine Eruption of Hunga Tonga-Hunga Ha'apai Volcano Provide an Excellent Research Opportunity. Earthquake Res. Adv., 100134